AIP | Journal of Applied Physics

Microstructural characteristics and phonon structures in luminescence from surface oxidized Ge nanocrystals embedded in HfO 2 matrix

S. Das, R. K. Singha, S. Gangopadhyay, A. Dhar, and S. K. Ray

Citation: Journal of Applied Physics **108**, 053510 (2010); doi: 10.1063/1.3475717
View online: http://dx.doi.org/10.1063/1.3475717
View Table of Contents: http://scitation.aip.org/content/aip/journal/jap/108/5?ver=pdfcov
Published by the AIP Publishing

Microstructural characteristics and phonon structures in luminescence from surface oxidized Ge nanocrystals embedded in HfO_2 matrix

S. Das,[1] R. K. Singha,[1] S. Gangopadhyay,[2] A. Dhar,[1] and S. K. Ray[1,a)]
[1]*Department of Physics and Meteorology, Indian Institute of Technology Kharagpur, Kharagpur 721302, India*
[2]*School of Physics and Astronomy, University of Nottingham, University Park, Nottingham NG7 2RD, United Kingdom*

(Received 1 May 2010; accepted 8 July 2010; published online 7 September 2010)

Ge nanocrystals embedded in HfO_2 matrices were prepared by rf magnetron sputtering technique. Transmission electron micrographs reveal the formation of spherical shape Ge nanocrystals of 4–6 nm diameters for 800 °C and 6–9 nm for 900 °C annealed samples. X-ray photoelectron spectroscopy confirms the formation of surface oxidized Ge nanocrystals. Embedded Ge nanocrystals show strong photoluminescence peaks in visible and ultraviolet region even at room temperature. Spectral analysis suggests that emission in 1.58 and 3.18 eV bands originate from $T_\Sigma(T_\Pi) \rightarrow S_0$, and $T'_\Pi \rightarrow S_0$ optical transitions in GeO color centers, respectively, and those in the range 2.0–3.0 eV are related to Ge/O defects at the interface of the oxidized nanocrystals. Temperature dependent photoluminescence study has revealed additional fine structures with lowering of temperature, the origin of which is attributed to the strong coupling of electronic excitations with local vibration of germanium oxides at the surface. © *2010 American Institute of Physics*. [doi:10.1063/1.3475717]

I. INTRODUCTION

The observations of visible photoluminescence (PL) from indirect band gap semiconductor nanocrystals such as Si or Ge, embedded in a dielectric matrix have potential applications for novel optical devices.[1] For Ge, most reports of visible and near-infrared PL from low-dimensional structures have involved Ge nanocrystals (NCs) embedded in SiO_2.[2–6] In comparison with Si, Ge has a larger effective Bohr radius for Wannier excitons (~23 nm), so it is much easier to change the electronic structure around the band gap of Ge. The light emission mechanism from Ge nanocrystals has been discussed extensively and was attributed either to radiative recombination via Ge quantum confined states[2–4,7] or to defects at the nanocrystals/matrix interface or in the matrix itself.[3,5,8] Therefore, the origin of visible PL of Ge nanocrystals embedded in a dielectric oxide matrix still remains to be clarified.

As the size of the nanocrystal decreases, the surface and interface atoms play more dominant role to determine the magnetic, optical, electrical, and electro-optical properties of the material due to large surface-to-volume ratio.[9,10] The coupling of electronic and vibrational excitations dramatically increases with the localization of excitons and quantum confinement in smaller dimensions.[11] This coupling has a significant influence on the optical and electrical properties of semiconductors, as it determines the transport behavior and energy relaxation rate of excited carriers.

Though a number of studies have been reported on the visible PL of Ge nanocrystals embedded in oxide matrix, there exists only one report showing the fine structures[12] in PL spectrum of Ge due to strong coupling of excitons. In this paper, we report the temperature dependent luminescence characteristics of oxidized Ge nanocrystals embedded in a high-permittivity HfO_2 matrix, which are useful for flash memory devices.[7] To our knowledge, this is the first report showing strong phonon peaks related to germanium oxide in luminescence spectrum of oxidized Ge nanocrystals. The strong coupling of electronic excitations with local vibrations of germanium oxides at the surface of the nanocrystals causes the evolution of observed fine structures.

II. EXPERIMENTAL

Luminescent nanocrystal Ge have been fabricated by several groups using cosputtering,[7,12] chemical vapor deposition,[13] ion implantation,[5] sol-gel,[14] and hydrothermal reduction in $Si_xGe_{1-x}O_2$.[15] In this study, Ge nanocrystals embedded in HfO_2 matrix on Si(100) substrates were deposited by radio frequency (13.56 MHz) magnetron cosputtering method similar to those reported earlier.[7,12] The structure consisted of a 40 nm Ge+HfO_2 film sandwiched between 5 nm buffer (on Si) and 15 nm capped HfO_2 layers. In order to grow Ge nanocrystals in HfO_2 matrix, the deposited film was thermally annealed in N_2 gas ambient for 30 min at 800 and 900 °C. For better understanding the samples detail are given in Table I. High-resolution transmission electron microscopy was carried out using a JEM 2100F (JEOL) field emission system with an operating voltage of 200 kV to probe the formation of Ge nanocrystals in the sandwiched structure. The surface and interfacial composition of Ge nanocrystals was analyzed by x-ray photoelectron spectroscopy (XPS) at a base pressure of 2×10^{-8} Torr, using a Kratos Axis Ultra spectrometer. The XPS study was carried out using a monochromated Al $K\alpha$ x-ray source, hybrid (magnetic/electrostatic) optics, a hemispherical analyzer, a

a)Electronic mail: physkr@phy.iitkgp.ernet.in.

TABLE I. Deposition parameters and postdeposition annealing conditions for Ge nanocrystals embedded in HfO_2.

	Deposition parameter			
Sample	Layer material	Substrate temperature	rf power (W)	Thickness (nm)
As-deposited	HfO_2	RT	50	5 ± 1
	$Ge+HfO_2$	RT	50	40 ± 2
	HfO_2	RT	50	15 ± 2
	Annealing condition			
		Temperature (°C)	Atmosphere	Time (min)
800 °C annealed		800	N_2	30
900 °C annealed		900	N_2	30

multichannel plate, and a delay line detector with a collection angle of 30° and a takeoff angle of 90°. PL spectra were recorded using a He–Cd laser as an excitation source, operating at 325 nm with an output power density of 1.3 W/cm^2 and a TRIAX 320 monochromator fitted with Hamamatsu R928 photomultiplier detector.

III. RESULTS AND DISCUSSION

A. Microstructural studies

TEM observation of the as-sputtered sample confirmed that the structure was completely amorphous with out the formation of Ge nanoclusters. Therefore, postdeposition annealing was carried out for nucleation of Ge nanocrystals in oxide matrix. Figure 1(a) shows a plain view TEM micrograph of sample annealed at 800 °C for 30 min in N_2 atmosphere. The dark patches seen are Ge nanocrystals of 4–6 nm diameters embedded in HfO_2 matrix. The nanocrystals are almost spherical and are well dispersed in the HfO_2 matrix. The selected area electron diffraction pattern in the inset of Fig. 1(a) reveals that these nanocrystals consist of cubic Ge in GeO_2 with tetragonal structure. Figure 1(b) shows the cross-sectional TEM micrograph of a sample annealed at 900 °C for 30 min. It shows the formation of Ge nanocrystals with diameters 6–9 nm. The inset of Fig. 1(b) shows clear lattice fringes, with a separation of 0.33 nm, which corresponds to the {111} plane of Ge with diamond structure. Figures 2(a) and 2(b) show the size distribution of the Ge nanocrystals for 800 and 900 °C annealed samples, respectively. The size distribution of the nanocrystals formed by annealing at 800 °C can be approximated by Gaussian nature with an average diameter of 5.2 nm. For the 900 °C annealed samples, the distribution of the nanocrystals throughout the film was not uniform. Fukada *et al.*[16] reported that the diffusion of Ge in SiO_2 and nucleation of Ge depend on the annealing temperature. It may be noted that the out-diffusion of Si from the substrate at elevated temperature enhances the nucleation and growth process of Ge nanocrystals at the $Si-SiO_2$ interface.[17] Ge nanocrystals usually show nonuniform distribution of size and density within SiO_2 due to the high diffusion rate of Ge atoms,[18] consistent with our observation for 900 °C annealed sample. Furthermore, a higher annealing temperature leads to an increase in the critical nucleus size, and would also raise the barrier for nucleation.[19]

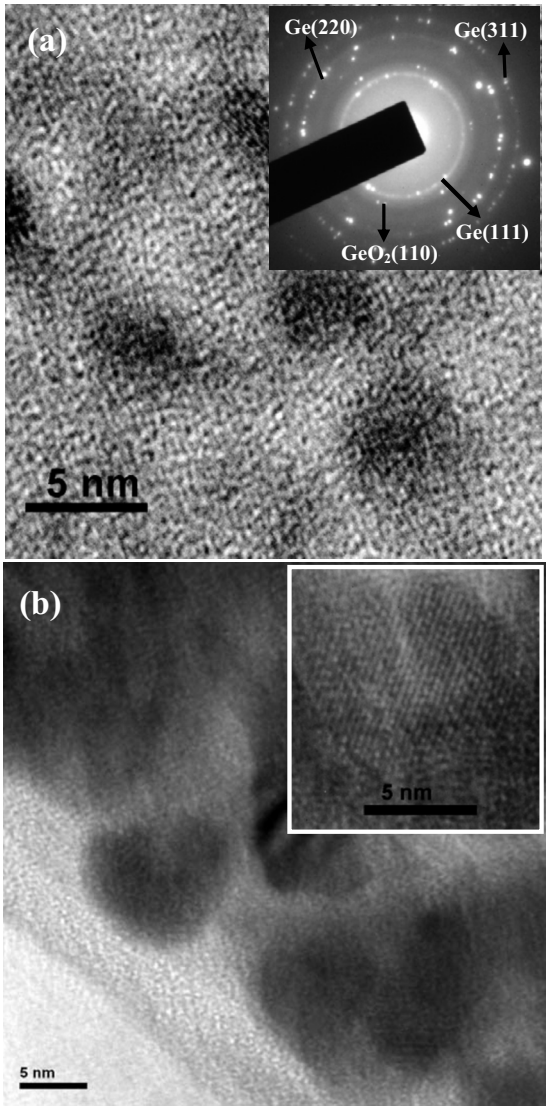

FIG. 1. TEM micrographs of Ge NCs embedded in HfO_2: (a) plan-view for 800 °C and (b) cross-sectional for 900 °C annealed samples.

B. Chemical bonding of surface oxidized Ge nanocrystals

Figure 3 shows the typical XPS spectra of Ge 3*d* core-level electron for 900 °C annealed sample at a depth of ~27 nm from the surface of the film. Five oxidation states, Ge^{n+} (n=0–4) responsible for the Ge 3*d* XPS peak could exist in Ge-embedded oxides.[20,21] The Ge 3*d* XPS peaks from elemental Ge (Ge^0) and GeO_2 are usually observed at ~29.1 eV and ~32.2 eV, respectively. The shift in the Ge 3*d* peak (with respect to Ge^0) has been attributed to Ge–O, Ge–Hf–O, and Ge–Hf bonds, as shown in the study of Ge suboxides[21,22] and Ge/HfO_2 interface.[22] The spectrum has been fitted by three peaks for germanium oxidation states.[23,24] The first one is assigned to the elemental Ge (Ge^0) around 29.1 eV and the other two are from oxide components. The Ge 3*d* peak with a chemical shift of 1.4 eV with

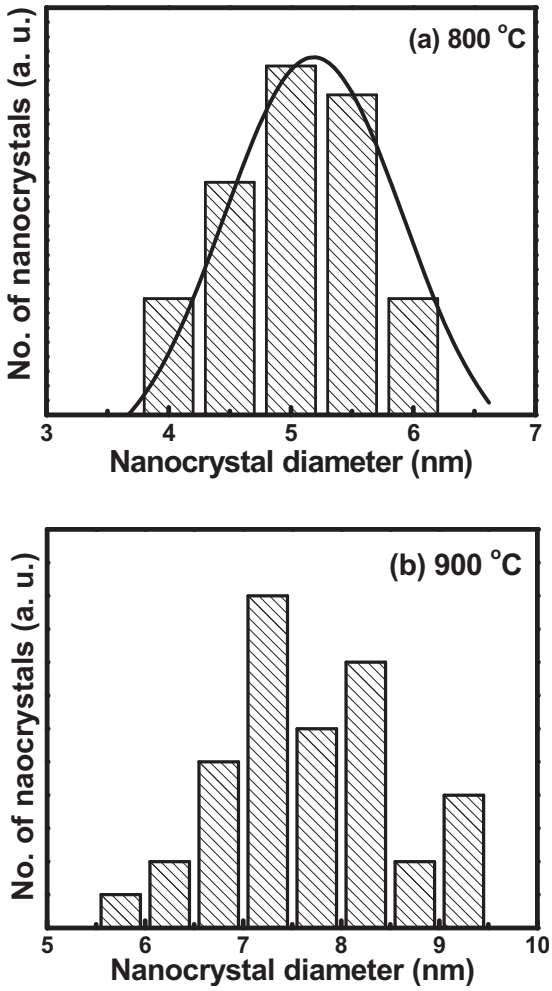

FIG. 2. Size distribution of Ge nanocrystals for (a) 800 °C and (b) 900 °C annealed samples.

respect to Ge^0 is related to Ge atoms in a 2+ oxidation state (GeO). The other peak is assigned to Ge atoms in a GeO_2-like environment with a 3.0 eV chemical shift. Ge^+ and Ge^{3+} states were not observed most probably due to

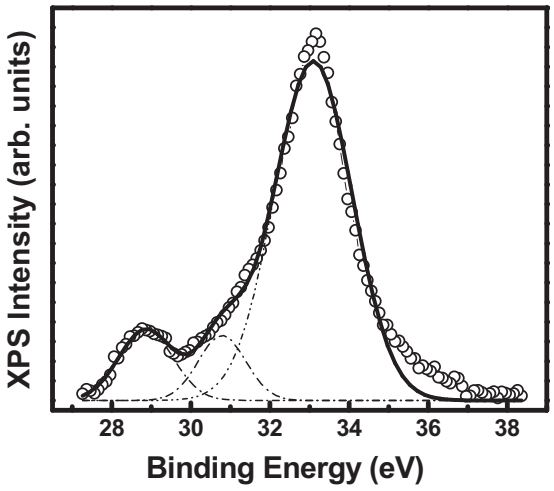

FIG. 3. Typical high-resolution Ge 3*d* XPS spectrum of 900 °C annealed sample at a depth 27 nm from the surface of the film. Deconvoluted XPS peaks of Ge 3*d* electron exhibit germanium oxides phases (GeO_2 and GeO) on the surface of Ge nanocrystals.

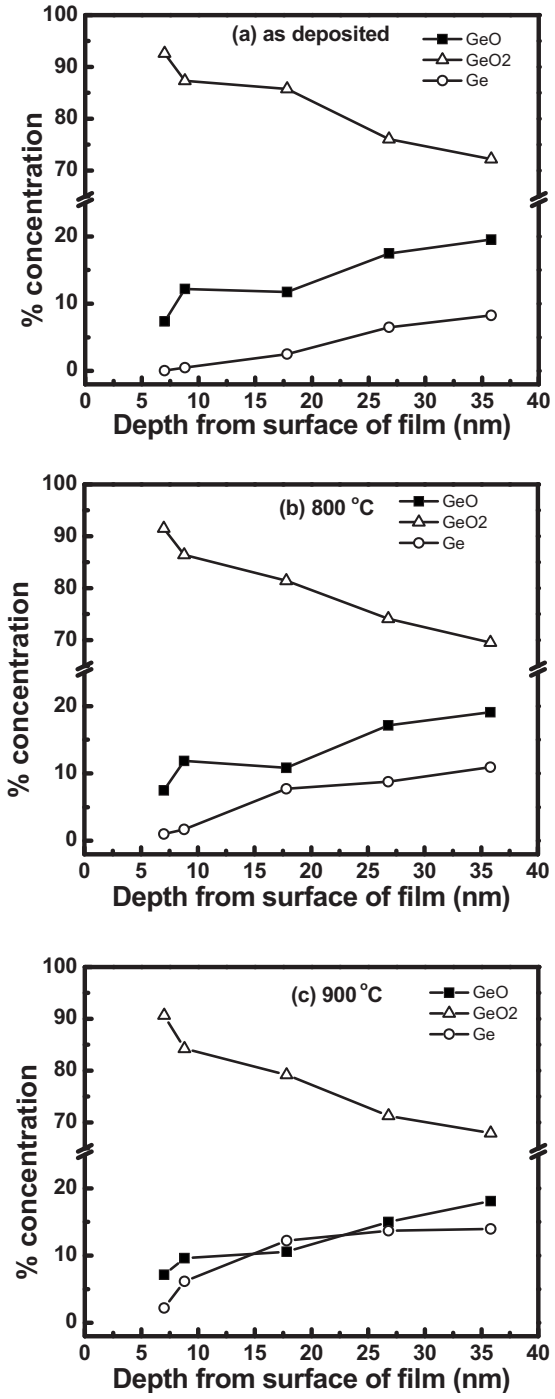

FIG. 4. Elemental concentration of Ge, GeO, and GeO_2 as a function of sample etch depth for the (a) as-sputtered, (b) 800 °C annealed, and (c) 900 °C annealed samples.

thermodynamic consideration, which rather favors Ge^{4+} and Ge^{2+} states. Figure 4(a) presents the elemental concentration of Ge, GeO, and GeO_2 as a function of sample etch depth for the as-sputtered sample. There is nearly no elemental Ge at a depth 7 nm from the surface of the film and the concentration increases from 0.5% to 8% for the depth varying from 8.8 to 35.8 nm. The concentration of GeO_2 reduces from 92% to 72% and that of GeO increases from 7% to 19%, as depth increases from 7.0 to 35.8 nm. The high proportion of GeO_2 and GeO in as-sputtered samples agree with those reported in Ge-embedded SiO_2.[25] The 800 °C annealed sample [Fig.

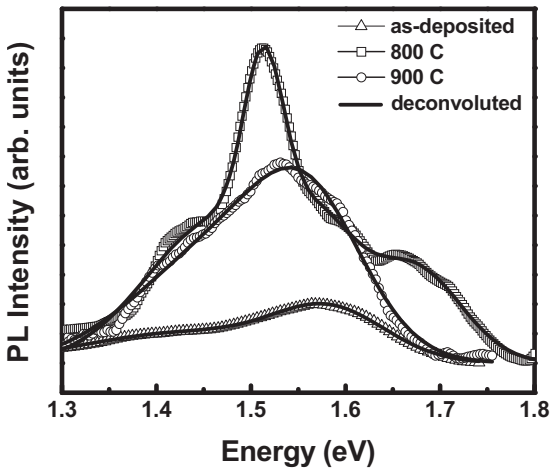

FIG. 5. Room temperature PL spectra of as-deposited and annealed (800 and 900 °C) samples in the photon energy range 1.3–1.75 eV.

4(b)] shows an increase in the Ge concentration from 1% to 11% as the depth increases from 7.0 to 35.8 nm. The concentration of GeO_2 is slightly lower than that of as-deposited sample (i.e., 91% and 69% at a depth 7.0 nm and 35.8 nm, respectively). On the other hand, GeO distribution remains nearly the same like to that of as-deposited film. Figure 4(c) shows a pronounced increase (2%–14%) in Ge concentration from a depth 7.0 to 35.8 nm for 900 °C annealed sample. A reduction in the concentrations of GeO_2 and GeO is observed compared to above results. The reduction in suboxides concentration leads to an increase in the Ge concentration in the film. Thus the formation of Ge nanocrystal most likely originates from the dissociation of suboxides and agglomeration of Ge during N_2 annealing.

C. PL studies

The PL characteristics of as-deposited and annealed samples have been studied in the photon energy range 1.30–3.50 eV and temperature range of 25–300 K using a He–Cd laser (wavelength 325 nm) as the excitation source. Figure 5 shows the room temperature PL spectra of as-deposited and annealed (800 and 900 °C) samples in the photon energy range 1.3–1.75 eV. All samples show broad PL in1.4–1.7 eV at room temperature. The PL spectrum of as-deposited sample has been decomposed into two Gaussian peaks centered at 1.43 and 1.58 eV. However for 800 °C annealed sample the PL spectrum can be represented by four Gaussians peaks centered at 1.46, 1.51, 1.57, and 1.67 eV. For 900 °C annealed sample the spectrum consists of two peaks centered at 1.47 and 1.56 eV. The red emission around 1.58 eV in all the samples is attributed,[26–28] to the optical excitation of the Ge-related oxygen-deficiency center into the first singlet state (S_1), followed by the intersystem crossing to the third triplet state (T'_π), and a radiative transition back to the ground state (S_0). Figures 6(a)–6(c) show the temperature dependent PL spectra of as-deposited, 800 °C, and 900 °C annealed sample, respectively, in the photon energy range 1.3 eV–1.75 eV. For all the samples we have observed PL thermal quenching. The observed thermal quenching of the PL signal is associated with the thermal dissociation of excitons. Interestingly, additional fine structures on the higher energy side of the ~1.58 eV PL peak appear at a low temperature for 800 and 900 °C annealed samples. These fine structures are related to phonon lines of GeO_2, which will be discussed in detail in Sec. IV. Different thermal quenching processes have been observed for different peaks. As the phonon related peaks originate due to coupling with the different types of phonon (TO or LO or A_1), they have different activation energies for thermal quenching, which are reflected in the temperature dependent PL spectrum.

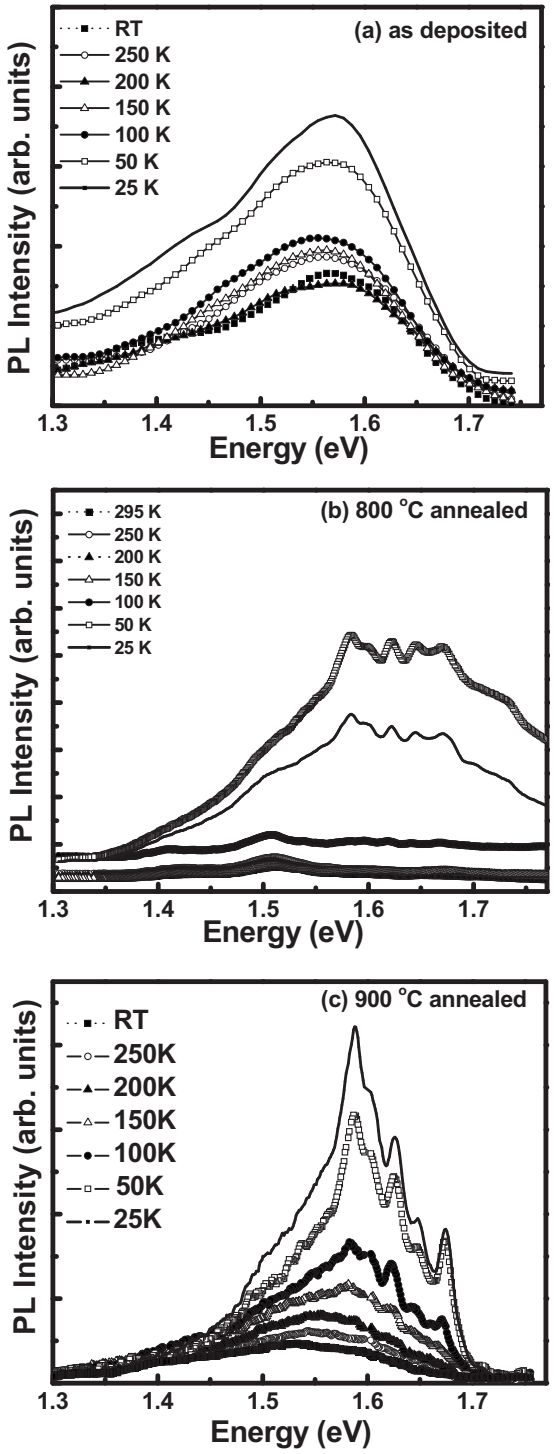

FIG. 6. Temperature dependent PL spectra of (a) as-deposited, (b) 800 °C annealed and (c) 900 °C annealed samples in the photon energy range 1.3–1.75 eV.

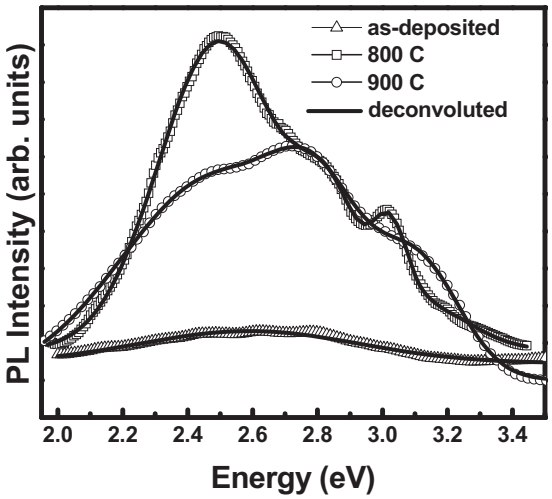

FIG. 7. Room temperature PL spectra of spectra of as-deposited and annealed (800 and 900 °C) samples in the photon energy range 2.5–3.5 eV.

Figure 7 shows the room temperature PL spectra of as-deposited and annealed samples in the photon energy range 2.5–3.5 eV. For as-deposited sample, we have observed a broad emission with a peak centered at 2.59 eV. For 800 °C annealed sample, the deconvoluted PL spectrum shows four Gaussians peaks centered at 2.49, 2.84, 3.02, and 3.11 eV. On the other hand the 900 °C annealed sample shows three peaks centered at 2.49, 2.81, and 3.11 eV. Temperature dependent PL characteristics have been studied to explain the origin of emission at different energies. Figures 8(a)–8(c) show the temperature dependent PL spectra of as-deposited, 800 °C, and 900 °C annealed sample, respectively. The 3.18 eV PL bands originated from Ge-doped SiO_2 have been reported previously,[26–28] which is attributed to GeO color centers. Optical transitions from the triplet state T_π or T_Σ to ground state (S_0) result in the 3.18 eV emission in GeO color centers, as predicted from the electronic state of GeO molecule.[27,28] The intensity of the PL peak around 3.18 eV for both the annealed sample increases rapidly on lowering the temperature. Interestingly, the additional fine structures on the higher energy side of the ~3.18 eV PL peak appear at low temperatures for both the annealed samples, but not in the as-deposited one. The PL peak around 2.5 eV for 800 °C annealed sample is redshifted and the peak intensity increases on lowering the temperature. This 2.5 eV peak emission is far away from the quantum confined PL of 5.2 nm Ge nanocrystals for 800 °C annealed sample. There are several reports of luminescence in the blue-green region with the peak energy independent of the size of the nanocrystals.[8,29,30] For example, Kartopu *et al.*[29] have reported a broad orange band between 2.6 and 1.5 eV attributed to defects in the GeO_x phase. Therefore, the observed PL bands in the energy range 2.0–2.8 eV originate owing to the radiative recombination through defects, which are located at the interface of the oxidized nanocrystals.

Figures 9(a) and 9(b) show PL spectra recorded at a typical low temperature (25 K) in more detail to explain the origin of fine structures. In Fig. 9(a), besides $T'_\Pi \rightarrow S_0$ (1.588 eV) transition in GeO molecule, additional fine structures are observed at 1.603, 1.627, 1.648, and 1.675 eV for both the

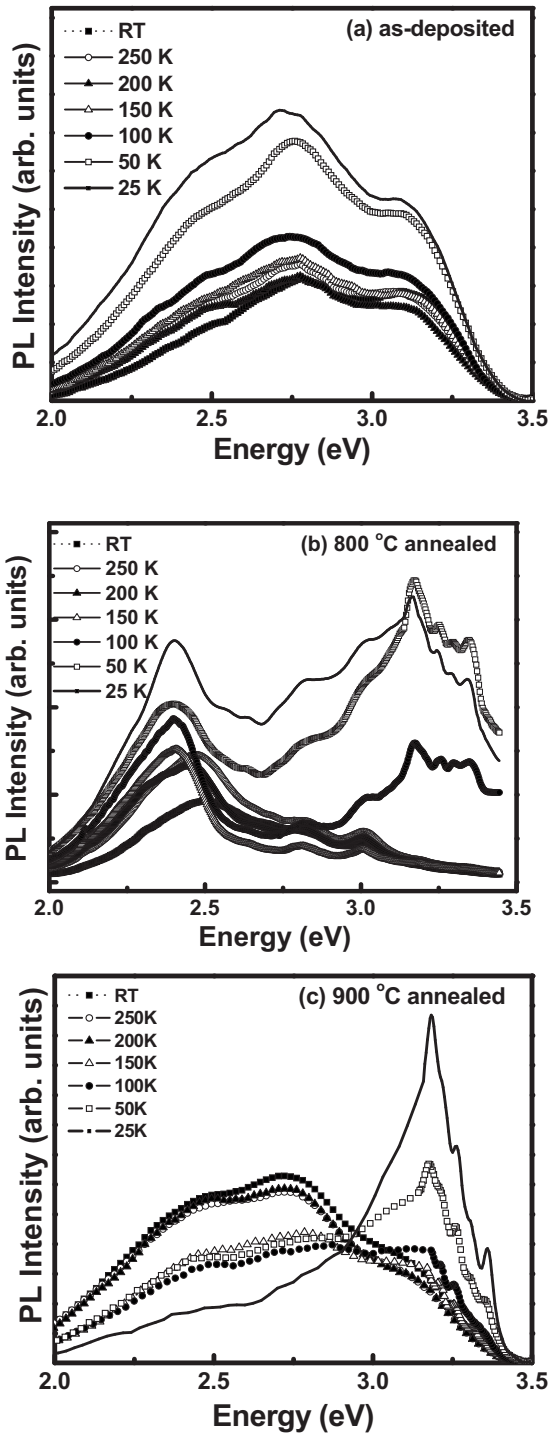

FIG. 8. Temperature dependent PL spectra of (a) as-deposited, (b) 800 °C annealed, and (c) 900 °C annealed samples in the photon energy range 2.5–3.5 eV.

annealed samples. Based on the observed temperature dependence and measured energy separation, the peaks are related to E(TO+LO), E(TO), E(TO), and E(TO)+A1 phonon lines of GeO_2 (Ref. 31) having energies 15 meV, 39 meV, 60 meV, and 87 meV, respectively. Similar phononlike structures are also observed on the higher energy side of the 3.184 eV $[T_\Sigma(T_\Pi) \rightarrow S_0]$ peak, as shown in Fig. 9(b). The additional spectral peaks are observed at 3.216, 3.262, 3.307, and 3.360 eV, which are related to 2E(TO+LO), 2E(TO), 2E(TO), and 2[E(TO)+A1] phonon lines of GeO_2 having energies 32

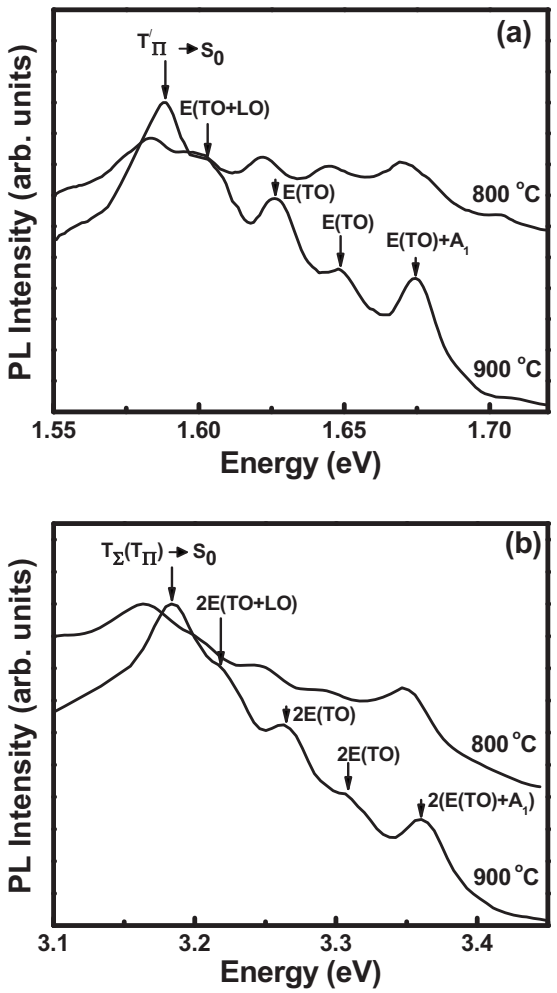

FIG. 9. Details of the phonon structures in PL spectra at 25 K around (a) 1.58 eV and (b) 3.18 eV.

meV, 78 meV, 123 meV, and 176 meV, respectively. For 800 °C annealed sample all the peaks are slightly redshifted (~16 meV) with respect to 900 °C annealed sample. This may be due to the different stress development in the surface oxidized nanocrystals. The observed phonon structure on the higher energy side of the excitonic peaks may be resulted from the simultaneous absorption of phonons and emission of photons in the annihilation process of exciton. Similar steplike phonon structures due to TO phonons are reported at low temperatures (<70 K) (Refs. 11 and 32) in porous Si. In porous silicon, the visible luminescence is originated due to high-level excitation in the Si–O–Si and/or SiH_x vibrational bands.[33] These experiments clearly showed the role of surface states and phonon assisted processes in the absorption and PL excitation spectra. The observed phonon structures in our low temperature PL spectra show that the interaction between electronic and localized vibrational excitations dominates the luminescence characteristics of surface oxidized Ge nanocrystals. Since the Ge–O bond is polar, the coupling of excitons and stretching vibrations of surface species increases with the localization of excitons in smaller dimensions. It is generally accepted that the exciton-phonon coupling is governed by two mechanisms: deformation potential and Fröhlich potential. The TO scattering is mainly determined by deformation potential related to short-range interaction. On the other hand, the LO scattering includes contributions from both Fröhlich potential and deformation potential. The relative strength between Fröhlich and deformation potential contribution depends strongly on the size of Ge nanocrystals.[34]

IV. CONCLUSIONS

In conclusion, we have synthesized Ge nanocrystals embedded in HfO_2 matrix sandwiched between HfO_2 layers by rf magnetron sputtering technique. XPS depth profile analysis has indicated the formation of surface oxidized Ge nanocrystals. Spectral analyses suggest that 1.58 eV and 3.18 eV PL bands originate from $T_{\Sigma}(T_{\Pi}) \rightarrow S_0$ and $T'_{\Pi} \rightarrow S_0$ optical transitions in GeO color centers, respectively, with their peak intensity enhanced at lower temperatures. Other two bands in the PL spectra in the energy range 2.0–3.0 eV are related to defects at the interface of the oxidized nanocrystals, with their peak intensity suppressed at a lower temperature. The observed strong phonon related peaks at low temperatures on the higher energy side of the excitonic peak are attributed to the strong coupling of surface localized excitons in the oxidized nanocrystals with local vibrations of germanium oxides.

ACKNOWLEDGMENTS

This work was supported by DRDO sponsored FIR project grant. The authors would like to acknowledge Professor Philip Moriarty for XPS measurements. One of the authors (S. Das) acknowledges the Council of Scientific and Industrial Research, Government of India, for awarding fellowship to carry out this work

[1] S. S. Iyer and Y. H. Xie, Science **260**, 40 (1993).
[2] Y. Maeda, Phys. Rev. B **51**, 1658 (1995).
[3] S. Takeoka, M. Fujii, S. Hayashi, and K. Yamamoto, Phys. Rev. B **58**, 7921 (1998).
[4] K. Choi, V. Ng, S. P. Ng, H. H. Thio, Z. X. Shen, and W. S. Li, J. Appl. Phys. **86**, 1398 (1999).
[5] K. S. Min, K. V. Shcheglov, C. M. Yang, A. Atwater, M. L. Brongersma, and A. Polman, Appl. Phys. Lett. **68**, 2511 (1996).
[6] S. K. Ray and K. Das, Opt. Mater. (Amsterdam, Neth.) **27**, 948 (2005).
[7] S. Das, K. Das, R. K. Singha, A. Dhar, and S. K. Ray, Appl. Phys. Lett. **91**, 233118 (2007).
[8] M. Zacharias and P. M. Fauchet, Appl. Phys. Lett. **71**, 380 (1997).
[9] Y. F. Zhang, Y. H. Tang, N. Wang, C. S. Lee, I. Bello, and S. T. Lee, Phys. Rev. B **61**, 4518 (2000).
[10] S. Okamoto and Y. Kanemitsu, Phys. Rev. B **54**, 16421 (1996).
[11] T. Suemoto, K. Tanaka, A. Nakajima, and T. Itakura, Phys. Rev. Lett. **70**, 3659 (1993).
[12] K. Das, M. NandaGoswami, R. Mahapatra, G. S. Kar, A. Dhar, H. N. Acharya, S. Maikap, J.-H. Lee, and S. K. Ray, Appl. Phys. Lett. **84**, 1386 (2004).
[13] A. K. Dutta, Appl. Phys. Lett. **68**, 1189 (1996).
[14] K. Das, V. Nagarajan, M. L. NadaGoswami, D. Panda, A. Dhar, and S. K. Ray, Nanotechnology **18**, 095704 (2007).
[15] D. C. Paine, C. Caragianis, T. Y. Kim, Y. Shigesato, and T. Ishahara, Appl. Phys. Lett. **62**, 2842 (1993).
[16] H. Fukuda, T. Kobayashi, T. Endoh, and Y. Ueda, Appl. Surf. Sci. **776**, 130 (1998).
[17] D. C. Paine, C. Caragianis, T. Y. Kim, Y. Shigesato, and T. Ishahara, Appl. Phys. Lett. **60**, 2886 (1992).
[18] X. L. Wu, T. Gao, X. M. Bao, F. Yan, S. S. Jiang, and D. Feng, J. Appl. Phys. **82**, 2704 (1997).
[19] W. K. Choi, V. Ho, V. Ng, Y. W. Ho, S. P. Ng, and W. K. Chim, Appl.

Phys. Lett. **86**, 143114 (2005).
[20]J. Żuk, H. Krzyżanowska, M. J. Clouter, M. Bromberek, H. Bubert, L. Rebohle, and W. Skorupa, J. Appl. Phys. **96**, 4952 (2004).
[21]G. Pourtois, M. Houssa, A. Delable, T. Conard, M. Caymax, M. Meuris, and M. M. Heyns, Appl. Phys. Lett. **92**, 032105 (2008).
[22]A. Molle, Md. N. K. Bhulyan, G. Tallarida, and M. Fanclulli, Appl. Phys. Lett. **89**, 083504 (2006).
[23]O. Renault, L. Fourdrinier, E. Martinez, L. Clavelier, C. Leroyer, N. Barrett, and C. Crotti, Appl. Phys. Lett. **90**, 052112 (2007).
[24]J. S. Hovis, R. J. Hamers, and C. M. Greenlief, Surf. Sci. **440**, L815 (1999).
[25]Y. Maeda, N. Tsukamoto, Y. Yazawa, Y. Kanemitsu, and Y. Masumoto, Appl. Phys. Lett. **59**, 3168 (1991).
[26]M. Gallagher and U. Österberg, Appl. Phys. Lett. **63**, 2987 (1993).
[27]V. O. Sokolov and V. B. Sulimov, Phys. Status Solidi B **186**, 185 (1994).
[28]J. K. Shen, X. L. Wu, R. K. Yuan, N. Tang, J. P. Zou, Y. F. Mei, C. Tan, X. M. Bao, and G. G. Siu, Appl. Phys. Lett. **77**, 3134 (2000).
[29]G. Kartopu, S. C. Bayliss, R. E. Hummel, and Y. Ekinci, J. Appl. Phys. **95**, 3466 (2004).
[30]M. Ardyanian, H. Rinnert, X. Devaux, and M. Vergnat, Appl. Phys. Lett. **89**, 011902 (2006).
[31]J. F. Scott, Phys. Rev. B **1**, 3488 (1970).
[32]Y. Kanemitsu and S. Okamoto, Phys. Rev. B **58**, 9652 (1998).
[33]R. P. Chin, Y. R. Shen, and V. Petrova-Koch, Science **270**, 776 (1995).
[34]M. Nirmal, C. B. Murray, and M. G. Bawendi, Phys. Rev. B **50**, 2293 (1994).